



A new rate equation model of continuous wave Tm:YAP laser

Yancheng Xia¹ · Chao Niu¹ · Kuan Li¹ · Shiwei Xue¹ · Yao Ma¹ · Chunting Wu¹

Received: 9 October 2023 / Accepted: 27 November 2023 / Published online: 27 December 2023
© The Author(s), under exclusive licence to Springer-Verlag GmbH Germany, part of Springer Nature 2023

Abstract

Novel theoretical model based on rate equations considering re-absorption is set up to deal with the output characteristics of continuous wave (CW) Tm: YAP laser for the first time. Compared with the model that ignore the reabsorption of thulium ion at all (Model 1) or only takes it as a fixed loss (Model 2), the simulation results of the new model (Model 3) can reflect the entire process of reabsorption more accurately and obtain numerical simulation results that are closer to experimental results. Laser characteristics of LD end-pumped CW Tm: YAP crystal is achieved experimentally, which can demonstrate the accuracy of the model. Output power of 7.1 W at 1936 nm is obtained with resonator length of 78 mm under the incident pump power of 27.13 W. While the simulation results on output power of Tm: YAP laser under incident pump power of 27.13 W and cavity length of 78 mm are 17.2 W, 2.76 W, 7.36 W for Model 1, 2, 3. The finding indicates that the new model can evaluate the output performance of Tm: YAP lasers in precise.

1 Introduction

2 μm laser, located in the atmospheric window and eye-safe band, has lots of applications, such as medical treatment, atmospheric remote sensing, material processing, nonlinear optical frequency conversion, and so on [1]. Laser diode pumped thulium ion (Tm^{3+}) doped crystals are the effective way to generate 2 μm laser [2], especially Tm^{3+} -doped yttrium aluminum oxide (YAP) crystal, which belongs to the space group D_{2h}^{16} , owns large effective emission cross-section, excellent thermal and mechanical properties and strong natural birefringence [3–5]. The establishment and

solution of rate equation model is an effective way to obtain the output performance of lasers, which can also lay a foundation for analyzing experimental phenomena. However, the existing rate equation model of Tm^{3+} doped lasers either ignore various effects [6–10], or regard those effects as a fixed loss [5, 7], which lead to significant deviation between experimental results and theoretical simulation results, thus losing the guiding significance of rate equation theory for conducting experiments.

The reabsorption in Tm^{3+} -doped laser was found and considered for the first time by Risk W P in 1988 [11], which was computer-only with no experiments. Then the upconversion loss and ground state loss of both Tm^{3+} and Ho^{3+} doped lasers were calculated by Rustad G et al. in 1996 [6]. In 1997, Taira T et al. made a great progress in quasi-three-level modeling [7]. In 2007, a more intuitive model was established by O.A. Burry et al. [5], for comparative analysis and optimization of Tm: YAG and Tm: YAP lasers, in which reabsorption is considered as a fixed loss and included in the loss coefficient γ . However, introducing reabsorption only as a loss into the rate equation, there may be significant deviations between the experimental results and the theoretical simulation results of Tm^{3+} -doped lasers. Although the reabsorption effect reduces the output power of the laser, the population inversion of the laser material increases to a certain extent, which means that a more accurate rate equation model is needed to describe the

✉ Yao Ma
mayao@cust.edu.cn

✉ Chunting Wu
bigsnow1@126.com

Yancheng Xia
1214937229z@gmail.com

Chao Niu
leoniuc@163.com

Kuan Li
2022100002@mails.cust.edu.cn

Shiwei Xue
xsweve@outlook.com

¹ Jilin Key Laboratory of Solid-State Laser Technology and Application, School of Physics, Changchun University of Science and Technology, Changchun, China

reabsorption process and improve the simulation accuracy of laser output performance.

In this paper, a new rate equation model of continuous wave (CW) Tm: YAP laser with fully consideration of reabsorption is developed. The models that ignore the reabsorption of thulium ion at all (Model 1) or only takes it as a fixed loss (Model 2) are also used to verify the advantage of the new model (Model 3). Laser performance of LD end-pumped CW Tm: YAP crystal is achieved experimentally to indicate the correctness of Model 3.

2 Energy level structure and transition of thulium ion

The quasi-three-level generation scheme of thulium laser is shown in Fig. 1.

The quasi-three-level generation scheme of thulium laser is shown in Fig. 1. The energy manifolds indicated 3H_4 , 3H_5 , 3F_4 and 3H_6 , recorded as by 4, 3, 2, 1. And because the lower laser level is one of the Stark sublevels of ground level, the generation scheme is a quasi-three-level. Tm^{3+} ions located at multiplet 1 will be extracted to manifold 4 after the absorption of pump photons, which can be expressed by pump rate R_p as formula (1).

$$R_p = \frac{P_a}{Al_a h \nu_p} \tag{1}$$

where h is Plank constant, ν_p is the frequency of pumping laser. P_a is the absorbed pumping power, connected with pumping power P_i that injected into the laser material, as $P_a = P_i(1 - \exp(-\sigma_a N_{Tm} l_a))$, in which σ_a is the absorption cross-section at the pumping wavelength, N_{Tm} is the thulium concentration, l_a is the length of the crystal. Thus, $1 - \exp(-\sigma_a N_{Tm} l_a)$ can be understood as an absorption ratio

of pump power. This idea of the ratio can also be used to describe the reabsorbed power of 1.9 μm laser. The pump laser can be seen as an ideal cylindrical light, whose mode cross-section A describes the space pumping laser passes, expressed by $A = \pi r_p^2$, in which r_p is the radius of the pumping beam.

Then Tm^{3+} ions on manifold 3H_4 will be downwards in three ways: spontaneous emission, thermal relaxation, and cross relaxation. The thermal relaxation assumed as instantaneous process can be ignored [7, 9]. An ion on manifold 3H_4 will interact with a surrounding ion on 3H_6 , one of them loses energy and another absorbs, both transition to 3F_4 , which can be shown as $({}^3H_4, {}^3H_6)$ to $({}^3F_4, {}^3F_4)$, and this process is the cross relaxation of Tm^{3+} -doped laser. Cross relaxation and the spontaneous emission determine the average lifetime of Tm^{3+} on manifold 3H_4 (t_4), which can be written as $t_4 = 0.541$ ms [12, 13]. To better illustrate the conjunction between t_4 and cross relaxation, cross relaxation rate γ_{cr} is introduced, expressed as formula (2).

$$\gamma_{cr} = \frac{1}{t_4} \left(\frac{N_{tm}}{N_0} \right)^2 \tag{2}$$

where N_0 is the thulium concentration at that the cross-relaxation rate is equal to the rate of the thulium ions transitions from multiplet 4 to the lower multiplets. γ_{cr} can be accurately calculated when taking $N_0 = 0.5$ at. % or other values around 0.5 at. % to 1.6 at. % [5, 12, 13]. N_0 is of great difficult to obtain [12, 13], however, γ_{cr} is mainly used for calculating quantum yield η_{QY} , and changing t_4 or N_0 would only make η_{QY} a variation from 1.88 to 2. Therefore, N_0 of 0.5 at. % and $t_4 = 0.541$ ms can be considered as an accurate hypothesis [5], which caused $\eta_{QY} = 1.972$ in the formula. Also, cross-relaxation of $({}^3H_5, {}^3H_6)$ to $({}^3F_4, {}^3F_4)$ is ignored due to the lifetime of 8 μs for multiplet 3H_5 . Also, $\beta_{43} = 0.55$, $\beta_{42} = 0.05$ here, and β_{41} is not involved in the rate equation [6].

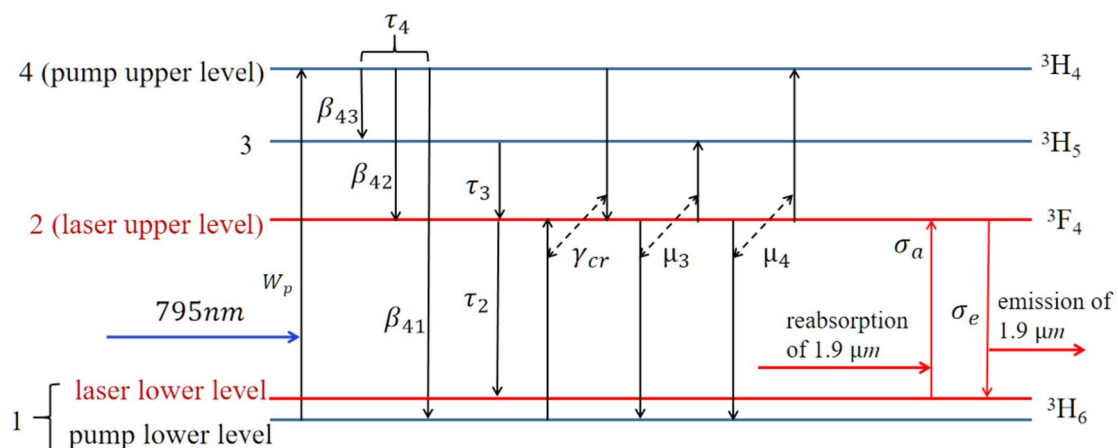


Fig. 1 Scheme of quasi-three-level thulium laser

Upconversion means the ions on multiplet 3F_4 may interact with each other, one of them loses energy and another absorbs, then transits to different multiplets, which degrades the laser performance. The value of the upconversion rate is denoted by μ_3 for (${}^3F_4, {}^3F_4$) to (${}^3H_5, {}^3H_6$) and μ_4 for (${}^3F_4, {}^3F_4$) to (${}^3H_4, {}^3H_6$). As the total upconversion rate is determined mainly by μ_3 , the value can be $\mu = 1.885 \times 10^{-18} \text{ cm}^3/\text{s}$ [5, 6].

As shown in Fig. 1, 1.9 μm radiative transition is generated between 3H_6 and 3F_4 Stark sub-level. Due to the laser photon energy is equal to the energy difference between 3H_6 and 3F_4 , the laser photon produced has a chance to be reabsorbed when counteracting with an ion on 3H_6 in Tm: YAP crystal, named reabsorption, which can be expressed as a rate. This can cause an increase of particle density on 3F_4 but a descend on 3H_6 , also the decrease of laser photons, which should be added in the model to describe the energy transfer process more precisely. Therefore, the reabsorption rate R_{re} can be expressed as formula (3).

$$\begin{cases} R_{re} = \frac{P_{io}(1 - \exp(-2\sigma_a N_{tm} l_a))}{A l_a h\nu} \\ \gamma_i = 2\sigma_a N_{tm} l_a \end{cases} \quad (3)$$

The P_{io} is the power of 1.9 μm laser oscillating in the resonator, which is expressed as:

$$P_{io} = \frac{h\nu}{t_r} q \quad (4)$$

where the value $t_r = 2L/c$ is the time of photons double passing along the resonator, q is number of photons. $P_{ao} = P_{io}(1 - \exp(-2\sigma_a N_{tm} l_a))$ is reabsorption ratio of laser photons, sharing the same structure in pump rate R , and the denominator of R_{re} is also the same to R . Considering the high reflectivity, and the laser keep generating along with pump light in the crystal, index ‘2’ in P_a and t_r is introduced here to describe laser double passing the resonator [5]. σ_a is absorption cross section on laser wavelength, which is $0.324 \times 10^{-21} \text{ cm}^2$ considering the experiments in this paper [5, 6, 14].

In formula (3), γ_i is reabsorption loss, often ignored (Model 1) or be taken as a fixed loss (Model 2) in previous works.

3 Novel theoretical model and simulations

A model considering the reabsorption as a rate can be expressed as formula (5).

$$\begin{cases} \frac{dN_4}{dt} = R + \mu_4 N_2^2 - \frac{N_4}{t_4} - \gamma_{cr} N_4 \\ \frac{dN_3}{dt} = \mu_3 N_2^2 + \beta_{43} \frac{N_4}{t_4} - \frac{N_3}{t_3} \\ \frac{dN_2}{dt} = 2\gamma_{cr} - 2(\mu_3 + \mu_4) N_2^2 + \frac{N_3}{t_3} + \beta_{42} \frac{N_4}{t_4} - \frac{N_2}{t_2} - \frac{c(\sigma_e N_2 - \sigma_a N_1)}{A l_a} q + R_{re} \\ N_{tm} = N_1 + N_2 + N_3 + N_4 \\ \frac{dq}{dt} = c(\sigma_e N_2 - \sigma_a N_1) q - \frac{q}{t_c} \end{cases} \quad (5)$$

where R_{re} is reabsorption rate. β_{4i} , in which $i = 1 \dots 3$ are the coefficients of luminescence branching, which indicates the destination of spontaneous emission by index ‘ i ’. q is a quantity of laser photons in cavity.

In formula (5), ignore R_{re} and change the expression of t_c , Model 1 can be obtained. It can delete R_{re} and only take the reabsorption as the loss to get Model 2. Reabsorption components, as reabsorption rate R_{re} and photon lifetime t_c , have been considered and circled in red, can be seen as Model 3, which actually express the essence of reabsorption, that ascend of population inversion and descend of photons in resonator. Reabsorption gain rate only appears in the dynamic equation describing N_2 , and the loss of reabsorption on the quantity of photons is already included in the photon lifetime t_c , which is expressed as $t_c = 2L/c\gamma$ in the model. γ is double-passing loss in the cavity, $\gamma = \gamma_i + (\gamma_1 + \gamma_2) + \gamma_L$. And $\gamma_i = 2\sigma_a N_{tm} l_a$ is the double-passing reabsorption loss. γ_1, γ_2 are losses of the mirrors, $\gamma_1 = -\ln(R_1), \gamma_2 = -\ln(R_2)$. γ_L is the cavity loss and can be taken as $\gamma_L = 0.015$ [7, 9].

Considering the concentrations of thulium ions on N_3 and N_4 are small enough, $N_{tm} = N_1 + N_2$. The density of inversion particles for quasi-three-level model is expressed as $N = N_2 - N_1 \sigma_a / \sigma_e$ [5], therefore, formula (6) is obtained (based on CW output).

$$\begin{cases} \eta_{QY} R - \frac{c\sigma_e}{A l_a} N q - \frac{N_2}{t_2} - \mu N_2^2 + R_{re} = 0 \\ \left(c\sigma_e N - \frac{1}{t_c} \right) q = 0 \end{cases} \quad (6)$$

Assuming $\eta_{QY} = \frac{\beta_{42} + \beta_{43} + 2\gamma_{cr} t_4}{1 + \gamma_{cr} t_4}$ as a quantum yield, $\eta_{QY} = 1.972$ after calculation. Thus, $\mu = \mu_3 + \mu_4(2 - \eta_{QY}) = 1.885 \times 10^{-18}$. It has been proved that quantum yield is close to 2 due to the existence of cross relaxation [5–7, 9].

The critical density of inversion particles N_c , the output laser power P_{re} (by solving formula (6) to obtain q) and the threshold pump power $P_{thresh_{re}}$ (by setting output power is 0 W) can be obtained after solving the Model 3, the results can be expressed as formula (7). It is different from the results of Model 2, as shown in formula (8), [5].

$$\begin{cases} N = \frac{1}{\frac{c\sigma_e t_c}{A l_a h\nu_p}} \\ P_{thresh_{re}} = \frac{A l_a h\nu_p}{\eta_{QY}(1 - \exp(-2\sigma_p N_{tm} l_a))} \left(\frac{N_2}{t_2} + \mu N_2^2 \right) \\ P_{re} = \frac{h\nu}{t_r} \gamma_2 \frac{A l_a t_r}{t_r - t_c (1 - \exp(-2\sigma_p N_{tm} l_a))} \left(\eta_{QY} \frac{P_i (1 - \exp(-2\sigma_p N_{tm} l_a))}{A l_a h\nu_p} - \frac{N_2}{t_2} - \mu N_2^2 \right) \end{cases} \quad (7)$$

$$\left\{ \begin{aligned} N &= \frac{1}{c\sigma_e t_c} \\ P_{\text{thres}} &= \frac{A_l h\nu_p}{\eta_{\text{QY}}(1-\exp(-2\sigma_p N_{\text{im}} l_a))} \left(\frac{N_2}{t_2} + \mu N_2^2 \right) \\ P &= \frac{h\nu l_2 A_l t_c}{t_r} \left(\eta_{\text{QY}} \frac{P_i(1-\exp(-2\sigma_p N_{\text{im}} l_a))}{A_l h\nu_p} - \frac{N_2}{t_2} - \mu N_2^2 \right) \end{aligned} \right. \quad (8)$$

And N_2 can be expressed as formula (9), works for both Model 1, 2 and 3, but t_c must be the respective expressions, same as other expressions including t_c .

$$N_2 = \frac{\sigma_a N_{\text{tm}} + \frac{1}{ct_c}}{\sigma_e + \sigma_a} \quad (9)$$

All parameters used are shown in Table 1.

Simulation on output power versus input pump power for Model 1, 2, and 3 is shown in Fig. 2.

The threshold is 2.75 W, 3.17 W and 3.18 W respectively, and the slope efficiency are 70.5%, 15.38% and 30.73% for Model 1, 2, and 3, respectively. The simulation result of Model 1 has a significant deviation from previous experimental reports [5, 6]. While, completely treating reabsorption as a loss can result in low slope efficiency of Tm: YAP laser, as Model 2. Therefore, it is necessary to comprehensively consider the impact of reabsorption on the output performance of Tm: YAP lasers in theory.

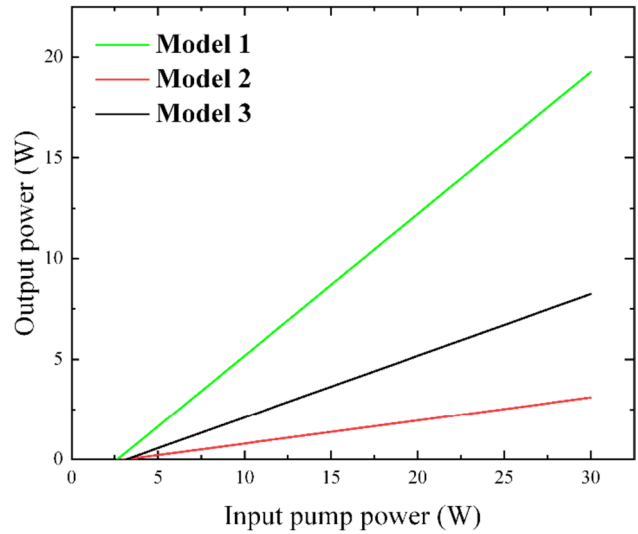


Fig. 2 Model simulation and comparison

4 Experimental results and analyses

To further demonstrate the accuracy of Model 3, experiment on laser characteristics of Tm: YAP crystal is carried out. The schematic of LD end-pumped Tm: YAP laser is shown in Fig. 3.

The pump source is a fiber coupled laser diode with central wavelength of 795 nm and maximum output power of 70 W. The radius and numerical aperture of the fiber are 200 μm and 0.22, respectively. The focus coupling ratio of the lens group is 1:1, and the focal lengths coated with

Table 1 The parameters used in the model [5, 6, 8, 9, 12, 14]

Parameter	Value
Plank constant (10^{-34} J·s)	6.626
Pump laser frequency (795 nm) (10^{14} Hz)	3.774
Output laser frequency (1936 nm) (10^{14} Hz)	1.54
Absorption cross-section on the pumping wavelength (10^{-21} cm ²)	9.1
Absorption cross-section on the laser-action wavelength (10^{-21} cm ²)	0.324
Stimulated emission cross-Sect. (10^{-21} cm ²)	5
Quantum efficiency	1.972
The upper laser level lifetime (10^{-3} s)	5
Total up-conversion loss constant (10^{-18} cm ³ /s)	1.885
Light speed in the crystal (10^{10} cm/s)	1.564
Refractive index of b-cut YAP crystal on the laser-action wavelength	1.9185
Thulium concentration (at. %)	3.5
Crystal length (mm)	14
Resonator length (mm)	78
Output mirror reflectivity	0.9
Cavity loss	0.015
Pumping beam radius (μm)	200

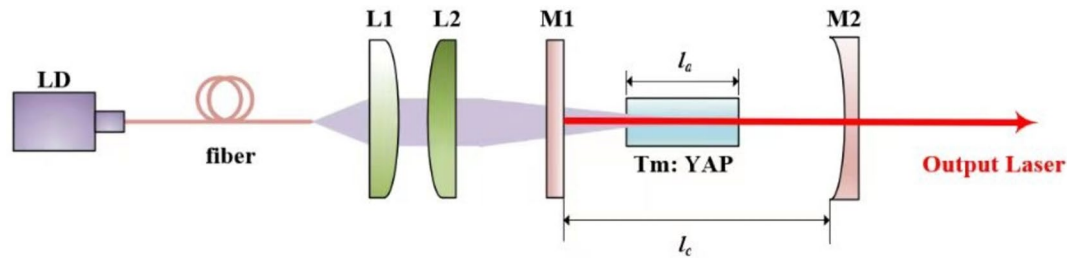


Fig. 3 Schematic of the LD end-pumped Tm: YAP laser

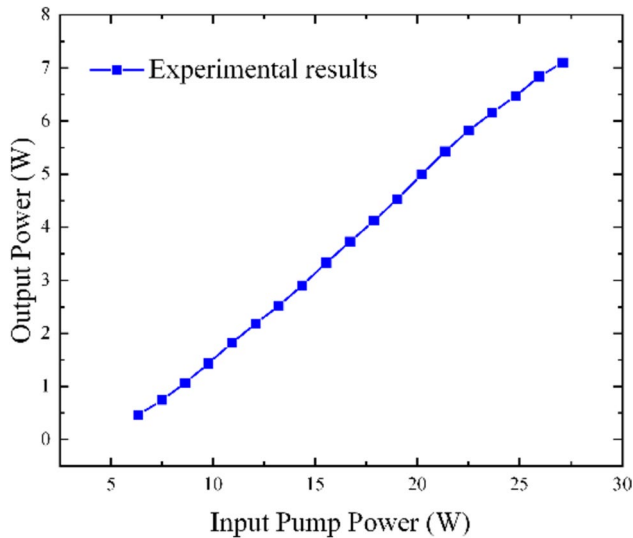


Fig. 4 Output power versus input power of Tm: YAP laser

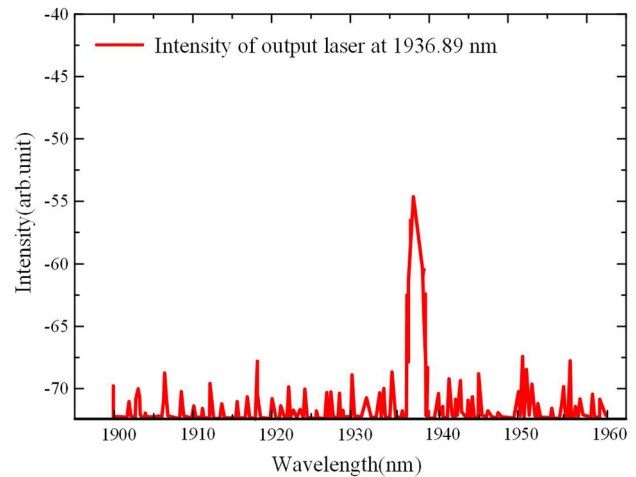


Fig. 5 Central wavelength of Tm: YAP laser

high transmissions at 795 nm ($T > 99.5\%$) are $f_1 = 35$ mm and $f_2 = 75$ mm, respectively. The mode matching between pump mode and laser mode is optimized by changing the pump beam waist radius and its location. M_1 is a plane mirror, coated with anti-reflection at 795 nm ($R < 0.5\%$) and high reflection ($R > 99.5\%$) at 1940 nm. M_2 is a concave output mirror with curvature radius of 200 mm and transmittance of 10% at 1940 nm. The Tm³⁺ doping concentration and the dimension of b-cut Tm: YAP crystal is 3.5 at. % and $\Phi 3 \times 14$ mm³, respectively. Both ends of the crystal are coated with anti-reflection at 795 nm ($R < 0.5\%$) and 1940 nm ($R < 0.5\%$). The crystal is wrapped in indium foil with the thickness of 0.05 mm and placed in a copper heat sink, which is cooled by water which is kept at 18 °C. The cavity length is 78 mm.

The output power versus input pump power is achieved, as shown in Fig. 4, by using a power meter F150A (OPHIR, Jerusalem, Israel). Threshold pump power of 5.19 W and maximum output power of 7.1 W under pump power of 27.13 W is obtained. The slope efficiency is 31.3%. However, saturation occurs at higher pump power. Higher pump

power means severely thermal accumulation in Tm: YAP crystal, leading to an enhancement of the upconversion of Tm: YAP, and a deterioration of the mode matching between pump mode and laser mode. The stability of the resonant cavity has changed, too.

The central wavelength of Tm: YAP laser is measured to be 1936.89 nm by a spectrometer (AQ6370 of Yokogawa, Musashino, Tokyo, Japan), as shown in Fig. 5.

The simulation results under Model 1, Model 2, Model 3, and experimental results are shown in Fig. 6.

The experimental threshold is 5.19 W, which is higher than that of 2.75 W, 3.17 W and 3.18 W for the simulation results of Model 1, 2, and 3. At pump power of 6.35 W, output power of 2.6 W, 0.37 W, 0.97 W and 0.46 W is obtained for simulation results of Model 1, 2, 3 and experimental result, which means the simulation results of Model 2 are closer to the actual situation at lower pump power. At pump power of 27.13 W, output power of 17.24 W, 2.76 W, 7.36 W is obtained for Model 1, 2, 3. While, the experimental result is 7.1 W, which is closer to the simulation result of Model 3. The deviation of the slope efficiency between the

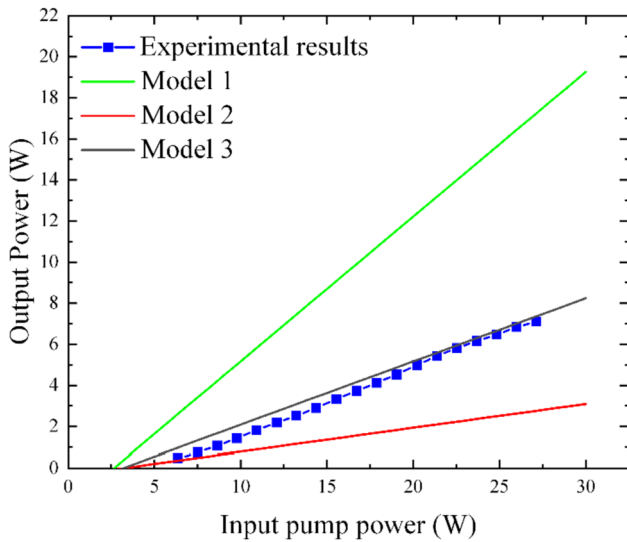


Fig. 6 Simulation results under three models and experimental results

simulation of Model 3 (30.73%) and experimental result (31.3%) is 0.57%. At low pump power, the photon density in the resonator is small, leads to lower probability of counteract between photons and thulium ions. As mentioned in formula (3), more q lead to higher R_{re} , which means Model 3 owns higher accuracy at high pump power.

The experimental results under resonator length of 51 mm and 105 mm are achieved, to further illustrate the accuracy of the Model 3.

As shown in Fig. 7, when the resonator length is 51 mm, the slope efficiency of experiment and Model 1, 2, 3 are

31.2%, 70.4%, 11.53%, 30.72%, respectively. And the slope efficiency under resonator length of 105 mm is 30.68%, 70.44%, 11.53%, 30.70%. As simulation results indicate, the three models exhibit similar slope efficiencies with different resonant cavity lengths. At the laser oscillation threshold, the output power in experiment is like the simulation result of Model 2, which means that when the pump power is low, the reabsorption loss has a more significant impact on the output power of the laser. While, beyond threshold, the output power in experiment is closer to the simulation results of Model 3, which means that considering reabsorption effect as a fixed loss is unreasonable. Deviation between experimental results and theoretical simulations mainly come from two aspects. The change in cavity length will lead to not only the changes in mode matching between the pump laser and the oscillating laser, but also the changes in the cavity loss. However, the slope efficiency of the experimental results is consistent with the simulation results of Model 3, which proves the accuracy of the model proposed in this paper.

5 Conclusion

In summary, a new theoretical model based on rate equations considering reabsorption is established to simulate the output characteristics of CW Tm: YAP laser more precisely for the first time. Compared to the model that completely ignore the reabsorption of thulium ion or only takes it as a fixed loss, the simulation results of the new model can better predict the output performance of Tm: YAP laser. Output power of 7.1 W at input pump power of 27.13 W

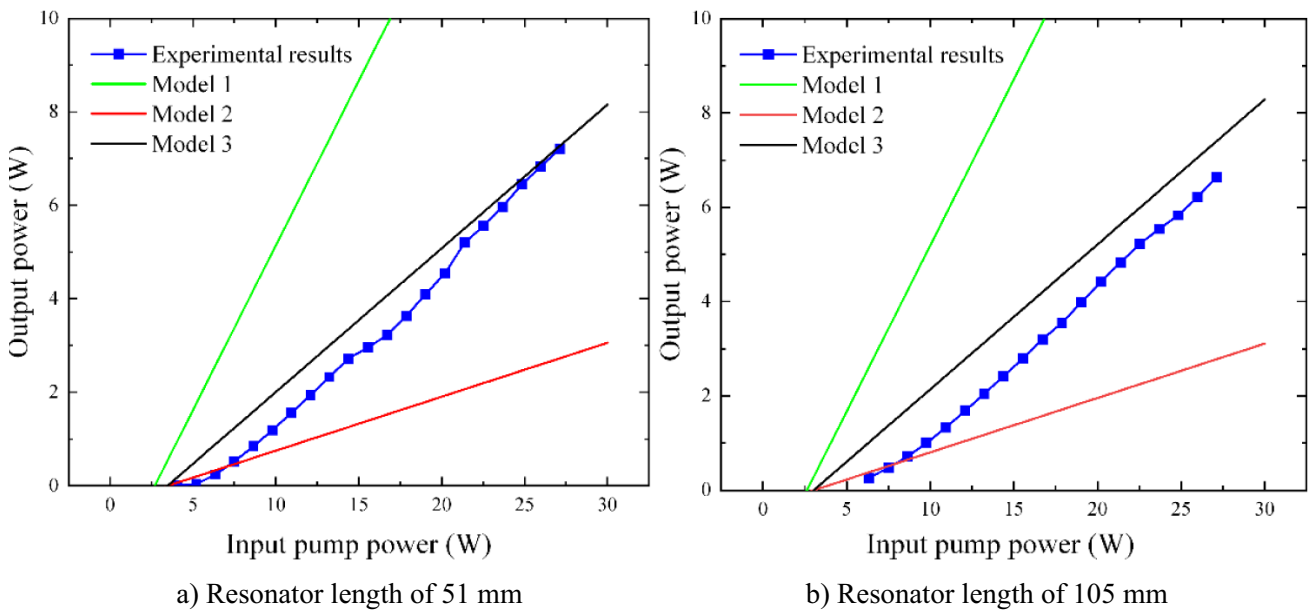


Fig. 7 Simulation results and experimental results with different resonator length

with resonator length of 78 mm is achieved in experiment, which is close to the simulation result of 7.36 W with the new model. The deviation of the slope efficiency between the simulation (30.73%) and experimental result (31.3%) is 0.57%. Experimental results with resonator length of 51 mm and 105 mm are obtained, which prove the accuracy of the model proposed in the paper. Further research can focus on refining each parameter, considering the field distribution of particles, and introducing Gaussian beams, to improve Model 3 and predict output transverse mode and longitudinal mode in simulation.

Acknowledgements This work was supported by Science and Technology Department of Jilin Province in China (Grant No. 20220402021GH).

Author contributions YX: completed the most of the article, including theoretical derivation, computer simulation, figure preparation, and some of the experiments. CN: helped with the experiments and process the experimental data. KL: prepared Fig. 1 and Fig. 4, and provided idea about experiments. SX: help wrote the main manuscript. CW and YM: as the mentors and corresponding authors, checked and revised the whole work.

Data availability The datasets generated and analyzed during the current study are available from the corresponding authors on reasonable request.

Declarations

Conflict of interest The authors declared that there is no conflict of interest.

References

1. J. Kwiatkowski, Power and spectral analyses in diode-pumped c-cut Pbnm Tm:YAP laser. *Chin Optics Lett.* **18**(09), 35–40 (2020)
2. A.O. Matkovskyy, *The materials of quantum electronics* (Liga-Press, Lviv, 2000). (In Ukrainian)
3. X.M. Duan, B.Q. Yao, G. Li et al., High efficient continuous wave operation of a Ho:YAP laser at room temperature. *Laser Phys. Lett.* **6**(4), 279–281 (2010)
4. L.I. Linjun, X. Yang, L. Zhou et al., Active/passive Q-switching operation of 2 μ m Tm, Ho:YAP laser with an acousto-optical Q-switch/MoS₂ saturable absorber mirror. *Photon Res* **6**(6), 614–619 (2018)
5. O.A. Buryy, D.Y. Sugak, S.B. Ubizskii et al., The comparative analysis and optimization of the free-running Tm³⁺:YAP and Tm³⁺:YAG microlasers[J]. *Appl. Phys. B* **88**(3), 433 (2007)
6. G. Rustad, K. Stenersen, Modeling of laser-pumped Tm and Ho lasers accounting for upconversion and ground-state depletion. *IEEE J. Quantum Electron.* **32**(9), 1645–1656 (1996). <https://doi.org/10.1109/3.535370>
7. T. Taira, W.M. Tulloch, R.L. Byer, Modeling of quasi-three-level lasers and operation of cw Yb:YAG lasers[J]. *Appl. Opt.* **36**(9), 1867–1874 (1997)
8. S.A. Payne, L.L. Chase, L.K. Smith et al., Infrared cross-section measurements for crystals doped with Er³⁺, Tm³⁺, and Ho³⁺. *IEEE J. Quantum Electron.* **28**(11), 2619–2630 (1992). <https://doi.org/10.1109/3.161321>
9. G.L. Zhu, Study on high repetition frequency Ho:YAP laser and its pump source Tm:YLF laser. *Harbin Inst Technol* (2012). <https://doi.org/10.7666/d.D241175>
10. X.M. Duan, Research on holmium single-doped oxide host solid-state laser at room temperature. *Harbin Inst Technol* (2012). <https://doi.org/10.7666/d.D241286>
11. W.P. Risk, Modeling of longitudinally pumped solid-state lasers exhibiting reabsorption losses. *J. Opt. Soc. Am. BOpt Soc Am B.* **5**(7), 1412–1423 (1988). <https://doi.org/10.1364/JOSAB.5.001412>
12. C. Honea Eric et al., 115-W Tm: YAG diode-pumped solid-state laser. *IEEE J. Quantum Electron.* **33**(9), 1592–1592 (1997)
13. J.M. O’Hare et al., Crystal-field determination for trivalent thulium in yttrium orthoaluminate. *Phys. Rev. B* **14**(9), 3732–3743 (1976). <https://doi.org/10.1103/physrevb.14.3732>
14. J.A. Caird, L.G. Deshazer, J. Nella, Characteristics of room-temperature 2.3- μ m laser emission from tm³⁺-in YAG and YAlO₃. *IEEE J. Quantum Electron.* **11**(11), 874–881 (2003). <https://doi.org/10.1109/JQE.1975.1068541>

Publisher’s Note Springer Nature remains neutral with regard to jurisdictional claims in published maps and institutional affiliations.

Springer Nature or its licensor (e.g. a society or other partner) holds exclusive rights to this article under a publishing agreement with the author(s) or other rightsholder(s); author self-archiving of the accepted manuscript version of this article is solely governed by the terms of such publishing agreement and applicable law.